Nonlinear Dyn (2009) 58: 237–248
DOI 10.1007/s11071-009-9474-3

ORIGINAL PAPER

Dynamics equations of a mobile robot provided with caster wheel

Stefan Staicu

Received: 10 March 2008 / Accepted: 27 January 2009 / Published online: 19 February 2009

Abstract Kinematics and dynamics of a mobile robot, consisting of a platform, two conventional wheels and a crank that controls the motion of a free rolling caster wheel, are analyzed in the paper. Based on several matrix relations of connectivity, the characteristic velocities and accelerations of this non-holonomic mechanical system are derived. Using the principle of virtual work, expressions and graphs for the torques and the powers of the two driving wheels are established. It has been verified the results in the framework of the second-order Lagrange equations with their multipliers. The study of the dynamics problems of the wheeled mobile robots is done mainly to solve successfully the control of the motion of such systems.

Keywords Dynamics · Kinematics · Mobile robot · Platform · Virtual work

Nomenclature

$Ox_0y_0z_0$	inertial reference frame with origin in the ground surface
$a_{k,k-1}$	orthogonal transformation matrix
$\vec{u}_1, \vec{u}_2, \vec{u}_3$	three right-handed orthogonal unit vectors
θ_1, θ_2	rotation angles of two driving wheels
θ_3	rotation angle of the caster wheel
ψ	rotation angle of the crank PO_3
l	distance between the wheel centers
$a+b$	height of the triangular platform
r	radius of each driving wheel
r_0	radius of the caster wheel
$\vec{r}_{21}^{\,A}, \vec{r}_{21}^{\,B}, \vec{r}_{32}^{\,C}$	relative position vectors of wheel centers
$\theta, x_{10}, y_{10}, H$	orientation angle and center coordinates of the moving platform
$\vec{\omega}_{k,k-1}$	relative angular velocity of T_k rigid body
$\vec{\omega}_{k0}$	absolute angular velocity of T_k
$\tilde{\omega}_{k,k-1}$	skew-symmetric matrix associated with the angular velocity $\vec{\omega}_{k,k-1}$
$\vec{\varepsilon}_{k,k-1}$	relative angular acceleration of T_k
$\vec{\varepsilon}_{k0}$	absolute angular acceleration of T_k
$\tilde{\varepsilon}_{k,k-1}$	skew-symmetric matrix associated with the angular acceleration $\vec{\varepsilon}_{k,k-1}$
$\vec{r}_k^{\,C}$	position vector of the mass center of T_k
$m_2^A, m_2^B, \hat{J}_2^A, \hat{J}_2^B$	mass and symmetric matrix of tensor of inertia of each driving wheel
$m_2^C, \hat{J}_2^C$	mass and tensor of inertia of the crank
$m_3^C, \hat{J}_3^C$	mass and tensor of inertia of the caster wheel
M_1, M_2	torques applied by two electric motors to the wheels jointed at A_2, B_2

S. Staicu (✉)
Department of Mechanics, University "Politehnica" of Bucharest, 313 Splaiul Independentei, Bucharest, Romania
e-mail: staicunstefan@yahoo.com

1 Introduction

The wheeled mobile robots are pre-programmable multi-functional systems with autonomous control designed to transport materials, parts, tools or specialized devices through variable programmed motions for performance in a variety of tasks. They consist of a mobile platform and a number of cylindrical wheels on a fixed or mobile surface, with rolling frictional motion. Such vehicles are used mainly in automated industrial processes.

The mobile robot is capable of autonomous motion because it is equipped with motors that are driven by an embarked computer. The concept of autonomy is understood as the ability to independently make intelligent decisions as the situation changes.

These machines are used in inaccessible environments that are often cluttered with unknown, moving or fixed obstacles, in agricultural works or in specialized medical procedures. This is why the study of the mobile robot dynamics acquires an increasing importance [1–3].

Wheeled mobile robots are a class of mechanical systems characterized by non-integrable kinematical constraints. The condition of rolling motion without slipping and side-slipping between the wheel and the contact surface demands the presence of non-holonomic constraints, which are the kinematic particularity of this kind of robot.

On the other hand, mobile robots are more complex to control than serial and parallel robots, because of non-holonomic constraints. But, at the level of instantaneous velocities, mobile robots can be treated mathematically as a special type of parallel robot, having different connections to the ground in parallel.

In his paper, Angeles [4] studied some interesting aspects of the mobile robot dynamics using the formalism of Lagrange equations. Other authors (e.g. Colbaugh et al. [5]) gave a characterization of the mechanical non-holonomic systems. Volterra, Appel and Ceaplighin used also the Lagrange equations and formalism of multipliers in the dynamics of motion with non-holonomic links. Recently, neural networks appeared as powerful tools for learning dynamic highly nonlinear systems (Kim et al. [6]).

The analysis of the problems of two-wheeled mobile robot dynamics is being done mainly to solve successfully the control of the motion of such systems. Simple models are very often accepted for a system description, even though they do not take into account the masses of the many mobile elements. Authors describing the dynamics of such systems use classical equations taken from Newtonian mechanics and, most often, they approach the motion of these systems using second-order Lagrange equations [7–10].

An equivalent parallel robot, consisting of three legs, can model a differentially driven mobile robot with two moving actuators [11, 12]. Pathak et al. [13] analyze the dynamic modeling and the position control of a series of wheeled inverted pendulums (Segway, Quasimoro, JOE) by partial feedback linearization and from a controllability point of view. Using recursive formulation, the kinematics model with a global singularity analysis is carefully discussed in [14]. Chakraborty and Ghosal have presented in their works [15, 16] the kinematics and a set of differential equations for the dynamics modeling and simulation of a wheeled mobile robot.

The Quasimoro prototype of the mobile wheeled-pendulum by Salerno and Angeles [17] is a special quasi-holonomic mechanical system which comprises two driving wheels and an intermediate central body carrying the payload. Salerno, Ostrovskaya and Angeles studied in the paper [18] the dynamics of a rolling robot, using the second-order Lagrange equations with multipliers.

In the present paper we establish an inverse dynamic model for the motion of a rolling robot provided with a caster wheel, using a matrix method based on the principle of virtual work. We will also determine the time-history evolution of the torques and the powers of the two active wheels.

2 Kinematics model of the robot

Let us consider a mobile robot with three conventional wheels that can roll without slipping on a horizontal surface (Fig. 1). This kind of differentially driven robots needs three non-collinear support points in order not to fall over. In practice, the robot can turn on the spot by giving opposite speeds to both actuated wheels.

The mobile robots are made up of a rigid frame with non-deformable wheels and sometimes they are moving on a fixed horizontal ground.

To simplify the graphical image of the kinematical scheme of the robot, in what follows we will represent the intermediate reference systems by only two

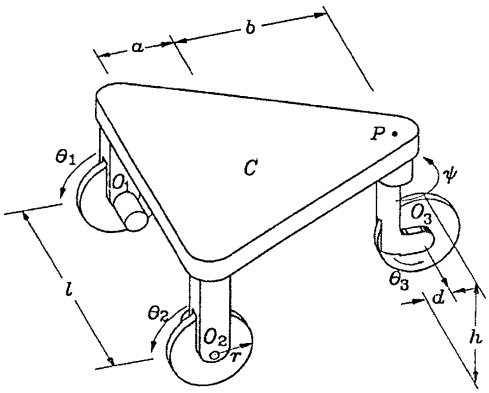

Fig. 1 General layout of wheeled mobile robot

axes, as is being presented in many robotics papers [4, 12, 25]. The z_k axis is represented for each component element T_k. It is noted that the relative rotation with the angle θ_i must be always about the direction of the z_k axis.

The moving platform of the robot, linked to a central reference frame $Gx_1y_1z_1$, is an isosceles triangle with the dimension $l$for the base and $a + b$ for its height. It has the mass m_1 and the tensor of inertia $\hat{J}_1$. Two cylindrical coaxial driving wheels of the same radius r are fixed to the frames $A_2x_2^Ay_2^Az_2^A$, $B_2x_2^By_2^Bz_2^B$ and connect to chassis by means of revolute joints at the points $A_2 = O_1$ and $B_2 = O_2$. They have the masses $m_2^A = m_2^B$ and the tensors of inertia $\hat{J}_2^A = \hat{J}_2^B$. A crank $C_2C_3 = PO_3$ is jointed to the moving platform at the point $C_2 = P$ of the triangle. Its mass and tensor of inertia with respect $C_2$are respectively m_2^C and $\hat{J}_2^C$. This rigid element can orientate permanently the motion of a passive rolling caster wheel of small a radius r_0, mass m_3^C and tensor of inertia $\hat{J}_3^C$ (Fig. 2). The caster wheel has no kinematical function; its only purpose is to keep the robot in balance.

Let us analyze now the motion of the robot on a curved trajectory in the turning period between two permanent rectilinear motions. The non-holonomic constraints reduce the mobile robot's velocity degrees of freedom and hence the robot has only two actuated joints.

In the forward velocity kinematics (FVK), we will consider that the input rotation angles θ_1, θ_2 of the driven wheels can determine completely the instantaneous position and orientation of the robot. Thus, since the platform has a planar motion, its position with respect to a fixed reference frame $Ox_0y_0z_0$ with origin

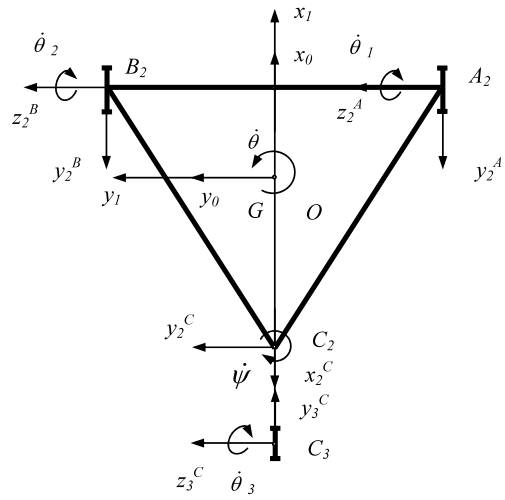

Fig. 2 Kinematical scheme of the mobile robot

O on the horizontal ground, is given by the coordinates x_{10}, y_{10}, H and by the angle of rotation θ, which form the following matrices:

$$\vec{r}_{10} = \begin{bmatrix} x_{10} \\ y_{10} \\ H \end{bmatrix}, \qquad a_{10} = \begin{bmatrix} \cos\theta & \sin\theta & 0 \\ -\sin\theta & \cos\theta & 0 \\ 0 & 0 & 1 \end{bmatrix}. \quad (1)$$

Let us denote by θ_i $(i = 1, 2, 3)$ the rotation angles of the three wheels and by $\theta_4 = \psi$ the relative angle of rotation of the crank about the apex C_2 of the platform.

In what follows, we apply the method of successive displacements to geometric analysis of closed-loop chains and we note that a joint variable is the displacement required to move a link from the initial location to the actual position. If every link is connected to at least two other links, the chain forms one or more independent closed loops. We call the matrix $a_{k,k-1}^{\varphi}$, for example, the orthogonal transformation 3×3 matrix of relative rotation with the angle $\varphi_{k,k-1}^A$ of link T_k^A around z_k^A axis.

In the study of the kinematics of mobile robots, we are interested to derive a matrix equation relating the location of an arbitrary T_k body to the joint variables. When the change of coordinates is successively considered, the corresponding matrices are multiplied. We obtain the following orthogonal transformation matrices in the reference frames [19]:

$$\begin{aligned} a_{21}^A &= a_z^{\theta_1} a_1, \qquad a_{21}^B = a_z^{\theta_2} a_1, \\ a_{21}^C &= a_z^{\theta_4} a_2, \qquad a_{32}^C = a_z^{\theta_3} a_1, \end{aligned} \quad (2)$$

where

$$a_1=\begin{bmatrix}0&0&-1\\-1&0&0\\0&1&0\end{bmatrix},\qquad a_2=\begin{bmatrix}-1&0&0\\0&1&0\\0&0&-1\end{bmatrix},$$
$$a_z^{\theta_1}=\begin{bmatrix}\cos\theta_i&\sin\theta_i&0\\-\sin\theta_i&\cos\theta_i&0\\0&0&1\end{bmatrix}\quad(i=1,2,3,4). \tag{3}$$

If the distance $A_2B_2=l$ between both actuated wheels is known, as well as the characteristic dimensions d, h of the crank PO_3, the following vectors give the invariable positions of the revolute joints A_2, B_2, C_2:

$$\vec{r}_{21}^{\,A}=\begin{bmatrix}a\\-l/2\\-h_0\end{bmatrix},\qquad \vec{r}_{21}^{\,B}=\begin{bmatrix}a\\l/2\\-h_0\end{bmatrix},$$
$$\vec{r}_{21}^{\,C}=\begin{bmatrix}-b\\0\\0\end{bmatrix},\qquad \vec{r}_{32}^{\,C}=\begin{bmatrix}d\\0\\h\end{bmatrix}. \tag{4}$$

So, the kinematics of the robot's elements is completely characterized by five relative angular velocities

$$\begin{aligned}&\vec{\omega}_{10}=\dot\theta\vec{u}_3,\qquad \vec{\omega}_{21}^{\,A}=\dot\theta_1\vec{u}_3,\\&\vec{\omega}_{21}^{\,B}=\dot\theta_2\vec{u}_3,\qquad \vec{\omega}_{21}^{\,C}=\dot\theta_4\vec{u}_3,\\&\vec{\omega}_{32}^{\,C}=\dot\theta_3\vec{u}_3,\qquad \vec{u}_3=[0\quad 0\quad 1]^T\end{aligned} \tag{5}$$

which are *associated* with the following skew-symmetric matrices:

$$\begin{aligned}&\tilde\omega_{10}=\dot\theta\tilde u_3,\qquad \tilde\omega_{21}^{A}=\dot\theta_1\tilde u_3,\qquad \tilde\omega_{21}^{B}=\dot\theta_2\tilde u_3,\\&\tilde\omega_{21}^{C}=\dot\theta_4\tilde u_3,\qquad \tilde\omega_{32}^{C}=\dot\theta_3\tilde u_3,\\&\tilde u_3=\begin{bmatrix}0&-1&0\\1&0&0\\0&0&0\end{bmatrix}.\end{aligned} \tag{6}$$

Since the analyzed system of three rolling wheels is characterized by non-holonomic constraints, *the matrix conditions of connectivity* (7) will establish five analytical relations between the characteristic velocities of a two-degrees-of-freedom mobile robot:

$$\begin{aligned}&\vec{v}_{10}+\tilde\omega_{10}\vec{r}_{21}^{\,A}=[r\dot\theta_1\quad 0\quad 0]^T\\&\vec{v}_{10}+\tilde\omega_{10}\vec{r}_{21}^{\,B}=[r\dot\theta_2\quad 0\quad 0]^T\\&a_{21}^{C}\big(\vec{v}_{10}+\tilde\omega_{10}\vec{r}_{21}^{\,C}\big)+\big(a_{21}^{C}\tilde\omega_{10}a_{21}^{C\,T}+\tilde\omega_{21}^{C}\big)\vec{r}_{32}^{\,C}\\&\quad=[-r_0\dot\theta_3\quad 0\quad 0]^T.\end{aligned} \tag{7}$$

These constraint conditions are satisfied if all wheels do not slip transversally and do not slip longitudinally, so that the distance over which the outer wheel surface rotates equals the distance traveled by the point on the rigid body to which the wheel axle is attached.

Indeed, we assume in *FVK* problem that the position and orientation of the mechanism at a given instant will be completely determined by the input rotation angles of the two actuated wheels, namely:

$$\begin{aligned}\theta_1&=\theta_1^*\Big[1-\cos\Big(\frac{\pi}{3}t\Big)\Big],\\\theta_2&=\theta_2^*\Big[1-\cos\Big(\frac{\pi}{3}t\Big)\Big].\end{aligned} \tag{8}$$

Therefore, the relations (7) can provide first the Jacobian matrix and then the expressions of the characteristic velocities of the moving platform:

$$\begin{aligned}&\omega_{10}=\dot\theta=\frac{r}{l}(\dot\theta_1-\dot\theta_2),\\&v_{10}^x=r\dot\theta_1-\frac{1}{2}l\dot\theta,\qquad v_{10}^y=-a\dot\theta,\\&[\dot x_{10}\quad \dot y_{10}\quad 0]^T=a_{10}^T[v_{10}^x\quad v_{10}^y\quad 0]^T.\end{aligned} \tag{9}$$

Concerning the kinematics of the crank PO_3 and the passive caster wheel jointed at the point $O_3=C_3$, from the matrix conditions (7) we will derive a significant differential equation and a relation containing the angular velocities $\omega_{21}^C=\dot\theta_4=\dot\psi$, $\omega_{32}^C=\dot\theta_3$ as follows:

$$\begin{aligned}&d\dot\psi+r\dot\theta_1\sin\psi-\big[d+0.5l\sin\psi+(a+b)\cos\psi\big]\dot\theta\\&\quad=0,\\&r_0\dot\theta_3=\big[(a+b)\sin\psi-0.5l\cos\psi\big]\dot\theta+r\dot\theta_1\cos\psi.\end{aligned} \tag{10}$$

In the forward position kinematics, the estimation of the relative angle of rotation ψ and the absolute pose of the moving platform must be performed by integration of the velocity equations (9), (10).

In order to determine new *conditions of connectivity* of the accelerations, we could derive the matrix relations (7). Thus, the characteristic accelerations of the moving platform are immediately obtained:

$$\begin{aligned}&\varepsilon_{10}=\dot\omega_{10}=\ddot\theta=\frac{r}{l}(\ddot\theta_1-\ddot\theta_2),\\&\gamma_{10}^x=r\ddot\theta_1+a\dot\theta^2-\frac{1}{2}l\ddot\theta,\\&\gamma_{10}^y=r\dot\theta\dot\theta_1-a\ddot\theta-\frac{1}{2}l\dot\theta^2,\\&[\ddot x_{10}\quad \ddot y_{10}\quad 0]^T=a_{10}^T[\gamma_{10}^x\quad \gamma_{10}^y\quad 0]^T.\end{aligned} \tag{11}$$

Note that the absolute velocities $\vec{v}_{k0}^{C}$, $\vec{\omega}_{k0}^{C}$, the accelerations $\vec{\gamma}_{k0}^{C}$, $\tilde{\varepsilon}_{k0}^{C}$ and the useful square matrices $\tilde{\omega}_{k0}^{C}\tilde{\omega}_{k0}^{C}+\tilde{\varepsilon}_{k0}^{C}$ of the third leg OC_2C_3 of the robot, for example, can be calculated with some recursive matrix formulae [20–22]:

$$
\begin{aligned}
&\vec{v}_{20}^{C}=a_{21}^{C}\{\vec{v}_{10}+\tilde{\omega}_{10}\vec{r}_{21}^{C}\},\\
&\vec{v}_{30}^{C}=a_{32}^{C}\{\vec{v}_{20}^{C}+\tilde{\omega}_{20}^{C}\vec{r}_{32}^{C}\},\\
&\vec{\omega}_{20}^{C}=a_{21}^{C}\vec{\omega}_{10}+\vec{\omega}_{21}^{C},\ \vec{\omega}_{30}^{C}=a_{32}^{C}\vec{\omega}_{20}^{C}+\vec{\omega}_{32}^{C},\\
&\vec{\gamma}_{20}^{C}=a_{21}^{C}\{\vec{\gamma}_{10}+(\tilde{\omega}_{10}\tilde{\omega}_{10}+\tilde{\varepsilon}_{10})\vec{r}_{21}^{C}\},\\
&\gamma_{30}^{C}=a_{32}^{C}\{\vec{\gamma}_{20}^{C}+(\tilde{\omega}_{20}^{C}\tilde{\omega}_{20}^{C}+\tilde{\varepsilon}_{20}^{C})\vec{r}_{32}^{C}\},\\
&\vec{\varepsilon}_{20}^{C}=a_{21}^{C}\vec{\varepsilon}_{10}+\vec{\varepsilon}_{21}^{C}+a_{21}^{C}\tilde{\omega}_{10}a_{21}^{CT}\vec{\omega}_{21}^{C},\\
&\vec{\varepsilon}_{30}^{C}=a_{32}^{C}\vec{\varepsilon}_{20}^{C}+\vec{\varepsilon}_{32}^{C}+a_{32}^{C}\tilde{\omega}_{20}^{C}a_{32}^{CT}\vec{\omega}_{32}^{C},\\
&\tilde{\omega}_{20}^{C}\tilde{\omega}_{20}^{C}+\tilde{\varepsilon}_{20}^{C}=a_{21}^{C}\{\tilde{\omega}_{10}\tilde{\omega}_{10}+\tilde{\varepsilon}_{10}\}a_{21}^{CT}\\
&\qquad\qquad+\tilde{\omega}_{21}^{C}\tilde{\omega}_{21}^{C}+\tilde{\varepsilon}_{21}^{C}+2a_{21}^{C}\tilde{\omega}_{10}a_{21}^{CT}\tilde{\omega}_{21}^{C},\\
&\tilde{\omega}_{30}^{C}\tilde{\omega}_{30}^{C}+\tilde{\varepsilon}_{30}^{C}=a_{32}^{C}\{\tilde{\omega}_{20}^{C}\tilde{\omega}_{20}^{C}+\tilde{\varepsilon}_{20}^{C}\}a_{32}^{CT}\\
&\qquad\qquad+\tilde{\omega}_{32}^{C}\tilde{\omega}_{32}^{C}+\tilde{\varepsilon}_{32}^{C}+2a_{32}^{C}\tilde{\omega}_{20}^{C}a_{32}^{CT}\tilde{\omega}_{32}^{C}.
\end{aligned}
\tag{12}
$$

3 Equations of motion

3.1 Principle of virtual work

Two electric motors that generate the torques $\vec{M}_1=M_1\vec{u}_3$ and $\vec{M}_2=M_2\vec{u}_3$, which have the direction of the common axis $A_2B_2=O_1O_2$, control the evolution of the driving wheels A_2, B_2 and transmit the motion at the passive caster wheel C_2.

We will study the *inverse dynamic problem*, in order to establish the variation of the torques M_1, M_2 and the powers P_1, P_2 developed by the two active wheels, during the evolution of the robot between the initial position and the other one, which corresponds to the stationary motion. Thus, we will use an approach based on the principle of virtual work.

In every analysis, the system is considered initially at rest. It is noteworthy that the simulation runs do not account for either external dissipation, such as rolling friction between the wheels and ground, or internal dissipation, such as friction in the bearings.

The fundamental principle of virtual work states that a mechanical system is under dynamic equilibrium if and only if the virtual work developed by all external, internal and inertia forces vanishes during any general virtual displacement, which is compatible with the kinematical constraints [4, 23, 25].

A first set of *virtual characteristic velocities* of the robot bodies results easily from the constraint conditions (7), namely:

$$
\begin{aligned}
&\omega_{1a}^{v}=1,\qquad \omega_{2a}^{v}=0,\qquad \omega_{10a}^{v}=\frac{r}{l},\\
&v_{10a}^{xv}=\frac{r}{2},\qquad v_{10a}^{yv}=-a\frac{r}{l},\\
&\omega_{3a}^{v}=\frac{r}{r_0}\left(\frac{1}{2}\cos\psi+\frac{a+b}{l}\sin\psi\right),\\
&\omega_{4a}^{v}=\frac{r}{d}\left(-\frac{1}{2}\sin\psi+\frac{a+b}{l}\cos\psi\right)+\frac{r}{l},\\
&\omega_{\varphi a}^{v}=\omega_{4a}^{v}-\omega_{10a}^{v}.
\end{aligned}
\tag{13}
$$

Assuming that the frictional forces at the joints are negligible, the virtual work produced by the forces of constraint at the joints is zero. Hence, the following compact expression of the torque applied to the right driving wheel A_2 (Staicu [24]) is:

$$
\begin{aligned}
M_1=&\,\vec{v}_{10a}^{vT}\vec{F}_{10}+\vec{\omega}_{10a}^{vT}\vec{M}_{10}\\
&+\vec{v}_{20a}^{AvT}\vec{F}_{20}^{A}+\vec{\omega}_{20a}^{AvT}\vec{M}_{20}^{A}+\vec{v}_{20a}^{BvT}\vec{F}_{20}^{B}\\
&+\vec{\omega}_{20a}^{BvT}\vec{M}_{20}^{B}+\vec{v}_{20a}^{CvT}\vec{F}_{20}^{C}\\
&+\vec{\omega}_{20a}^{CvT}\vec{M}_{20}^{C}+\vec{v}_{30a}^{CvT}\vec{F}_{30}^{C}+\vec{\omega}_{30a}^{CvT}\vec{M}_{30}^{C}
\end{aligned}
\tag{14}
$$

with its analytical form

$$
\begin{aligned}
M_1=&\,m_1\omega_{10a}^{v}\left(\frac{1}{4}l^2\ddot{\theta}-\frac{1}{2}lr\ddot{\theta}_1-ar\dot{\theta}\dot{\theta}_1+a^2\ddot{\theta}\right)\\
&+m_1\omega_{1a}^{v}\left(r^2\ddot{\theta}_1-\frac{1}{2}lr\ddot{\theta}+ar\dot{\theta}^2\right)+J_1^{z}\ddot{\theta}\omega_{10a}^{v}\\
&+\frac{1}{2}m_2^{A}r^2\left(3\omega_{1a}^{v}\ddot{\theta}_1+\frac{1}{2}\omega_{10a}^{v}\ddot{\theta}\right)\\
&+\frac{1}{2}m_2^{B}r^2\left(3\omega_{2a}^{v}\ddot{\theta}_2+\frac{1}{2}\omega_{10a}^{v}\ddot{\theta}\right)\\
&+m_2^{C}\omega_{3a}^{v}r_0\left[r_0\ddot{\theta}_3-\left(d-x_2^{C}\right)\omega_{\varphi}^{2}\right]\\
&+m_2^{C}\omega_{\varphi a}^{v}\left[r_0\left(d+x_2^{C}\right)\dot{\theta}_3\omega_{\varphi}+\frac{d^3(3h+d)}{3(h+d)}\varepsilon_{\varphi}\right]\\
&+\frac{1}{2}m_3^{C}r_0^{2}\left(3\omega_{3a}^{v}\ddot{\theta}_3+\frac{1}{2}\omega_{\varphi a}^{v}\varepsilon_{\varphi}\right),
\end{aligned}
\tag{15}
$$

where $\omega_{\varphi}=\dot{\psi}-\dot{\theta}$, $\varepsilon_{\varphi}=\ddot{\psi}-\ddot{\theta}$.

The force of inertia and the resultant moment of the forces of inertia have, for example, the following general form:

$$\begin{aligned} -\vec{F}_{k0}^{inC} &= -m_k^C\{\vec{\gamma}_{k0}^C + (\tilde{\omega}_{k0}^C\tilde{\omega}_{k0}^C + \tilde{\varepsilon}_{k0}^C)\vec{r}_k^C\} \\ -\vec{M}_{k0}^{inC} &= -\{m_k^C\tilde{r}_k^C\vec{\gamma}_{k0}^C + \hat{J}_k^C\vec{\varepsilon}_{k0}^C + \tilde{\omega}_{k0}^C\hat{J}_k^C\vec{\omega}_{k0}^C\}, \end{aligned} \tag{16}$$

where the accelerations $\vec{\gamma}_{k0}^C$, $\vec{\varepsilon}_{k0}^C$ and the square matrices $\tilde{\omega}_{k0}^C\tilde{\omega}_{k0}^C + \tilde{\varepsilon}_{k0}^C$ can be calculated by relations (12).

For the torque M_2 of the couple applied to the left driving wheel B_2, an expression analogous to (15) results in

$$\begin{aligned} M_2 = {} & m_1\omega_{10b}^v\left(\frac{1}{4}l^2\ddot{\theta} + \frac{1}{2}lr\ddot{\theta}_2 - ar\dot{\theta}\dot{\theta}_2 + a^2\ddot{\theta}\right) \\ & + m_1\omega_{2b}^v\left(r^2\ddot{\theta}_2 + \frac{1}{2}lr\ddot{\theta} + ar\dot{\theta}^2\right) + J_1^z\ddot{\theta}\omega_{10b}^v \\ & + \frac{1}{2}m_2^B r^2\left(3\omega_{2b}^v\ddot{\theta}_2 + \frac{1}{2}\omega_{10b}^v\ddot{\theta}\right) \\ & + \frac{1}{2}m_2^A r^2\left(3\omega_{1b}^v\ddot{\theta}_1 + \frac{1}{2}\omega_{10b}^v\ddot{\theta}\right) \\ & + m_2^C\omega_{3b}^v r_0\left[r_0\ddot{\theta}_3 - \left(d - x_2^C\right)\omega_\varphi^2\right] \\ & + m_2^C\omega_{\varphi b}^v\left[r_0\left(d + x_2^C\right)\dot{\theta}_3\omega_\varphi + \frac{d^3(3h+d)}{3(h+d)}\varepsilon_\varphi\right] \\ & + \frac{1}{2}m_3^C r_0^2\left(3\omega_{3b}^v\ddot{\theta}_3 + \frac{1}{2}\omega_{\varphi a}^v\varepsilon_\varphi\right), \end{aligned} \tag{17}$$

where the following virtual velocities must be introduced:

$$\begin{aligned} & \omega_{1b}^v = 0, \qquad \omega_{2b}^v = 1, \qquad \omega_{10b}^v = -\frac{r}{l}, \\ & v_{10b}^{xv} = \frac{r}{2}, \qquad v_{10b}^{yv} = a\frac{r}{l}, \\ & \omega_{3b}^v = \frac{r}{r_0}\left(\frac{1}{2}\cos\psi - \frac{a+b}{l}\sin\psi\right), \\ & \omega_{4b}^v = -\frac{r}{d}\left(\frac{1}{2}\sin\psi + \frac{a+b}{l}\cos\psi\right) - \frac{r}{l}, \\ & \omega_{\varphi b}^v = \omega_{4b}^v - \omega_{10b}^v. \end{aligned} \tag{18}$$

The matrix relation (14) constitutes the *inverse dynamic model* of the mobile robot provided with caster wheel.

The various dynamical effects, including the Coriolis, coupling centrifugal forces and the gravitational actions, are considered in this explicit equation.

3.2 The Lagrange Equations

A solution of the dynamics problem of the mobile robots can be developed based on the Lagrange equations of second kind. Considering the non-holonomic constraints, the moving mechanism is a mechanical system of two degrees of freedom. The generalized coordinates of the robot are represented by seven parameters: $q_1 = x_{10}$, $q_2 = y_{10}$, $q_3 = \theta$, $q_4 = \theta_1$, $q_5 = \theta_2$, $q_6 = \theta_3$, $q_7 = \psi$.

The Lagrange equations with their multipliers $\lambda_1, \lambda_2, \ldots, \lambda_5$ will be expressed by seven differential relations:

$$\frac{d}{dt}\left\{\frac{\partial E}{\partial\dot{q}_k}\right\} - \frac{\partial E}{\partial q_k} = Q_k + \sum_{s=1}^{5}\lambda_s c_{sk} \quad (k = 1, 2, \ldots, 7). \tag{19}$$

Five kinematical conditions of constraint given by (7):

$$\sum_{k=1}^{7} c_{sk}\dot{q}_k = 0 \quad (s = 1, 2, \ldots, 5) \tag{20}$$

can be concentered in a matrix form, as follows:

$$C\dot{\bar{q}} = 0, \tag{21}$$

where

$$C = \begin{bmatrix} \cos\theta & \sin\theta & l/2 & -r & 0 & 0 & 0 \\ \cos\theta & \sin\theta & -l/2 & 0 & -r & 0 & 0 \\ -\sin\theta & \cos\theta & a & 0 & 0 & 0 & 0 \\ -\cos\varphi & \sin\varphi & -b\sin\psi & 0 & 0 & r_0 & 0 \\ \sin\varphi & \cos\varphi & -(d + b\cos\psi) & 0 & 0 & 0 & d \end{bmatrix},$$

$$\dot{\bar{q}} = [\dot{x}_{10} \quad \dot{y}_{10} \quad \dot{\theta} \quad \dot{\theta}_1 \quad \dot{\theta}_2 \quad \dot{\theta}_3 \quad \dot{\psi}]^T, \tag{22}$$

$$\varphi = \psi - \theta.$$

The components of the general expression of kinetic energy $E = \sum_{j=1}^{5} E_j$ are expressed as analytical functions of the generalized coordinates and their first derivatives with respect to time:

$$\begin{aligned} E_1 &= \frac{1}{2}m_1\left(\dot{x}_{10}^2 + \dot{y}_{10}^2\right) + \frac{1}{2}J_1^z\dot{\theta}^2, \\ E_2 &= \frac{1}{2}m_2^A\left[\left(\dot{x}_{10}\cos\theta + \dot{y}_{10}\sin\theta + \frac{l}{2}\dot{\theta}\right)^2 \right. \\ &\quad \left. + (-\dot{x}_{10}\sin\theta + \dot{y}_{10}\cos\theta + a\dot{\theta})^2\right] \end{aligned}$$

$$
\begin{aligned}
&+\frac{1}{8}m_2^A r^2\left(\dot\theta^2+2\dot\theta_1^2\right),\\
E_3=&\frac{1}{2}m_2^B\left[\left(\dot x_{10}\cos\theta+\dot y_{10}\sin\theta-\frac{l}{2}\dot\theta\right)^2\right.\\
&\left.+(-\dot x_{10}\sin\theta+\dot y_{10}\cos\theta+a\dot\theta)^2\right]\\
&+\frac{1}{8}m_2^B r^2\left(\dot\theta^2+2\dot\theta_2^2\right),\\
E_4=&\frac{1}{2}m_2^C\left[(\dot x_{10}\cos\theta+\dot y_{10}\sin\theta)^2\right.\\
&\left.+(-\dot x_{10}\sin\theta+\dot y_{10}\cos\theta-b\dot\theta)^2\right]\\
&+m_2^C(\dot x_{10}\sin\varphi+\dot y_{10}\cos\varphi-b\dot\theta\cos\psi)x_2^C\dot\varphi\\
&+\frac{1}{6}m_2^C\frac{d^3}{h+d}\dot\varphi^2,\\
E_5=&\frac{1}{2}m_3^C\left[(-\dot x_{10}\cos\varphi+\dot y_{10}\sin\varphi-b\dot\theta\sin\psi)^2\right.\\
&\left.+(\dot x_{10}\sin\varphi+\dot y_{10}\cos\varphi-b\dot\theta\cos\psi+d\dot\varphi)^2\right]\\
&+\frac{1}{8}m_3^C r_0^2\left(\dot\varphi^2+2\dot\theta_3^2\right).
\end{aligned}
\tag{23}
$$

A long and tedious calculus of the partial derivatives of the above functions leads to an algebraic system of seven relations. In the inverse dynamics problem, after elimination of the five multipliers, finally we can obtain the same expressions as (15), (17) for the torques M_1, M_2 required by the two driving wheels.

If the above complete equations (15), (17) do not take into account the small masses of the caster wheel C_3 and the crank C_2C_3, the expression of the torques M_1, M_2 for a symmetrical mobile robot can be written in the simplified form:

$$
\begin{aligned}
M_1=&m_1r^2\left[\frac{1}{4}(\ddot\theta_1+\ddot\theta_2)+\frac{a^2}{l^2}(\ddot\theta_1-\ddot\theta_2)\right.\\
&\left.-\frac{ar}{l^2}\dot\theta_2(\dot\theta_1-\dot\theta_2)\right]\\
&+\frac{1}{2}m_2^A r^2\left[3\ddot\theta_1+\frac{r^2}{l^2}(\ddot\theta_1-\ddot\theta_2)\right]\\
&+J_1^z\frac{r^2}{l^2}(\ddot\theta_1-\ddot\theta_2),\\
M_2=&m_1r^2\left[\frac{1}{4}(\ddot\theta_1+\ddot\theta_2)+\frac{a^2}{l^2}(\ddot\theta_2-\ddot\theta_1)\right.\\
&\left.-\frac{ar}{l^2}\dot\theta_1(\dot\theta_2-\dot\theta_1)\right]\\
&+\frac{1}{2}m_2^A r^2\left[3\ddot\theta_2+\frac{r^2}{l^2}(\ddot\theta_2-\ddot\theta_1)\right]\\
&+J_1^z\frac{r^2}{l^2}(\ddot\theta_2-\ddot\theta_1).
\end{aligned}
\tag{24}
$$

After the comparison with the simplified results (24), we note that the dynamical equations of motion based on Maggie's approach or Lagrange's formalism obtained by J. Giergiel, W. Zylski ([7]; pp. 513 and 517) and Z. Hendzel ([8]; p. 852) are all unfortunately erroneous.

4 Dynamic simulations

As application, one will analyze the motion of a robot which has the following characteristics:

$$
\begin{aligned}
&x_2^C=\frac{1}{2}\frac{d^2}{(h+d)},\qquad J_1^z=\frac{1}{3}m_1l^2,\\
&m_1=10\text{ kg},\qquad m_2^A=m_2^B=2\text{ kg},\\
&m_2^C=1\text{ kg},\qquad m_3^C=0.25\text{ kg},\\
&l=0.5\text{ m},\qquad a=l\frac{\sqrt{3}}{6},\qquad b=2a,\\
&d=0.025\text{ m},\qquad r=0.1\text{ m},\qquad r_0=0.025\text{ m},\\
&h_0=0.2\text{ m},\qquad H=h_0+r,\qquad h=H-r_0.
\end{aligned}
\tag{25}
$$

Three important manoeuvres can be implemented.
1. *Rectilinear translation*. Considering two equal kinematics inputs,

$$
\begin{aligned}
&\theta_1^*=\theta_2^*=\frac{\pi}{2},\qquad x_{10}=r\theta_1,\qquad y_{10}=0,\\
&\theta=0,\qquad \psi=0,\qquad \theta_3=\frac{r}{r_0}\theta_1,
\end{aligned}
\tag{26}
$$

the center G of the platform moves along the direction of the fixed axis x_0 with a variable acceleration. The first and second derivatives of input angles are equal, since the load conditions have a symmetrical representation. Also, the other positional parameters are held equal to zero.

The two driving wheels are actuated by equal torques:

$$
M_1=M_2=\frac{1}{2}r^2\ddot\theta_1\left(m_1+3m_2^A+m_2^C+\frac{3}{2}m_3^C\right).
\tag{27}
$$

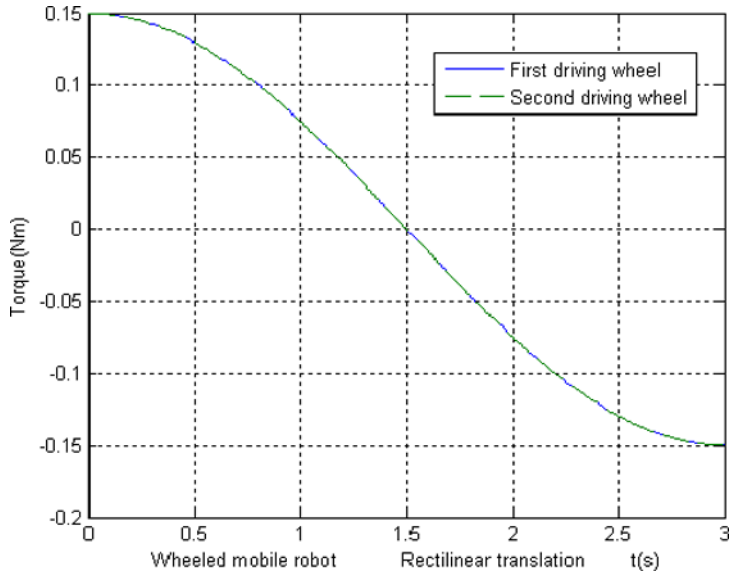

Fig. 3 Rectilinear translation: torques of driving wheels

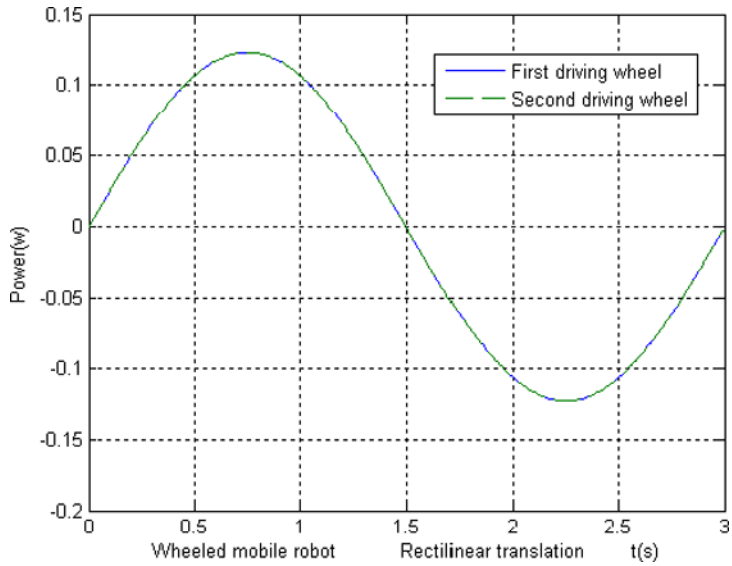

Fig. 4 Rectilinear translation: powers of driving wheels

As can be seen from Figs. 3 and 4, it is proved to be true that the torques and powers of the driving wheels are permanently equal one to another.

If the masses of the ensemble crank–caster wheel are supposed negligible, we obtain the known expression

$$M_1 = M_2 = \frac{1}{2} r^2 \ddot{\theta}_1 \left(m_1 + 3m_2^A\right). \tag{28}$$

2. *Rotation motion* about the vertical axis passing through the midpoint of the actuated wheel axle A_2B_2, with

$$\begin{aligned} &\theta_1^* = -\theta_2^* = \frac{\pi}{2}, \\ &v_{10}^x = 0, \qquad v_{10}^y = -2a\frac{r}{l}\dot{\theta}_1, \\ &\dot{\theta} = 2\frac{r}{l}\dot{\theta}_1. \end{aligned} \tag{29}$$

Starting from initial position, the crank and the caster wheel first have a transition motion. Angular ve-

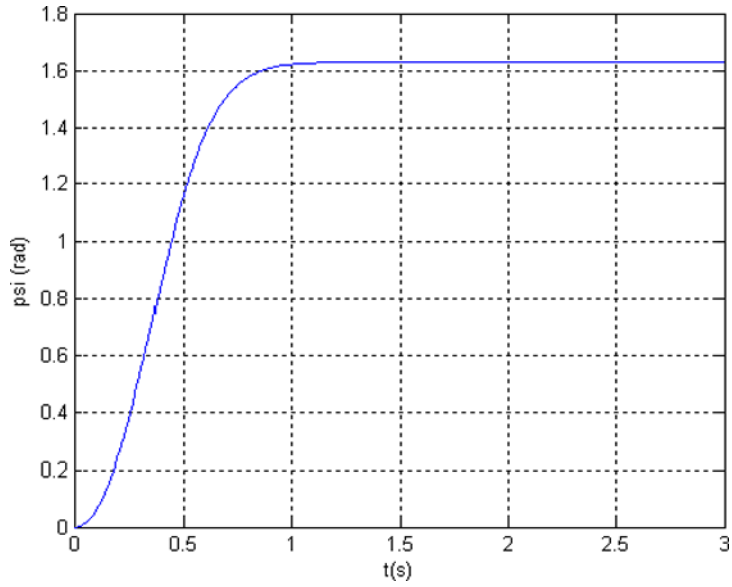

Fig. 5 Rotation angle ψ in transition period

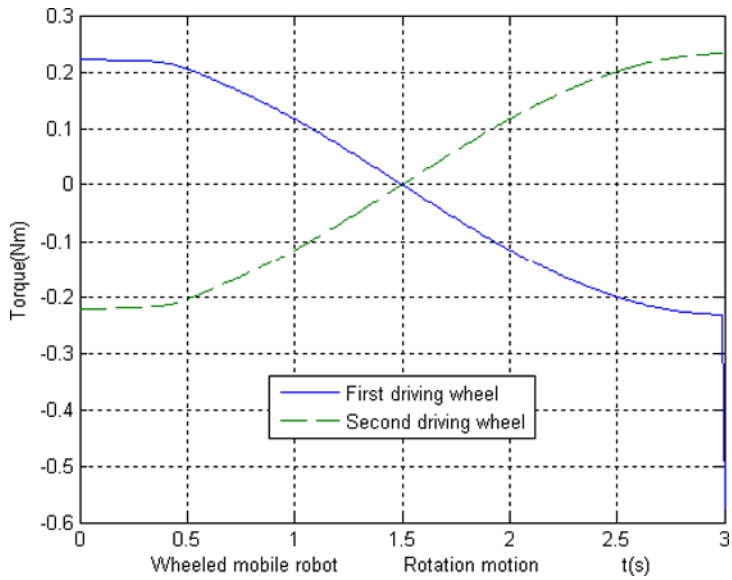

Fig. 6 Rotation motion: torques of driving wheels

locities $\dot{\psi}$, $\dot{\theta}_3$ follow two functions:

$$\dot{\psi} = \left(1 + \frac{a+b}{d}\cos\psi\right)\dot{\theta}, \qquad \dot{\theta}_3 = \frac{a+b}{r_0}\dot{\theta}\sin\psi. \tag{30}$$

We remark a quick increase of the relative angle ψ (Fig. 5) and vanishing of the velocity $\dot{\psi}$ to a characteristic angle ψ_0, as follows:

$$\cos\psi_0 = -\frac{d}{a+b}. \tag{31}$$

In a stabilized rotation, the center C_3 describes a circle of radius $R = (a+b)\sin\psi_0$ with an angular velocity

$$\dot{\theta}_3 = \frac{R}{r_0}\dot{\theta}. \tag{32}$$

Introducing in (15) and (17) a new set of virtual velocities

$$\omega^v_{1a} = 1, \qquad \omega^v_{2a} = 0, \qquad \omega^v_{10a} = \frac{r}{l}, \qquad \omega^v_{3a} = \frac{R}{r_0}\omega^v_{10a}, \qquad \omega^v_{\varphi a} = -\omega^v_{10a} \tag{33}$$

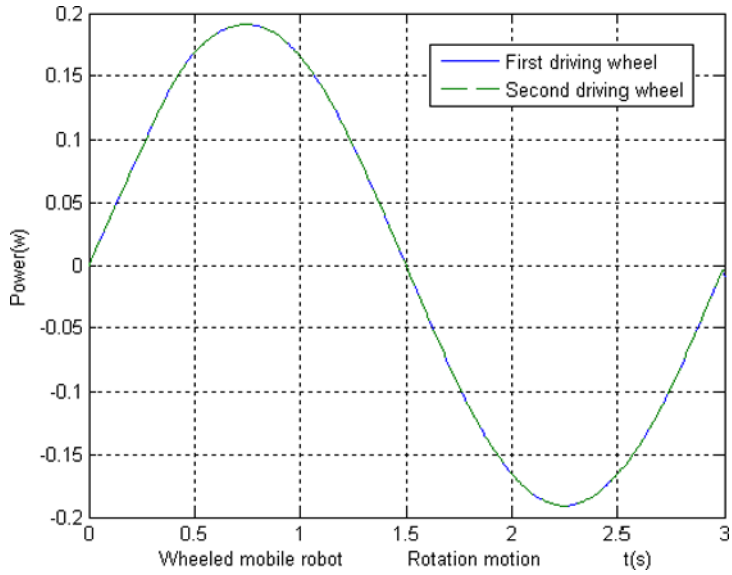

Fig. 7 Rotation motion: powers of driving wheels

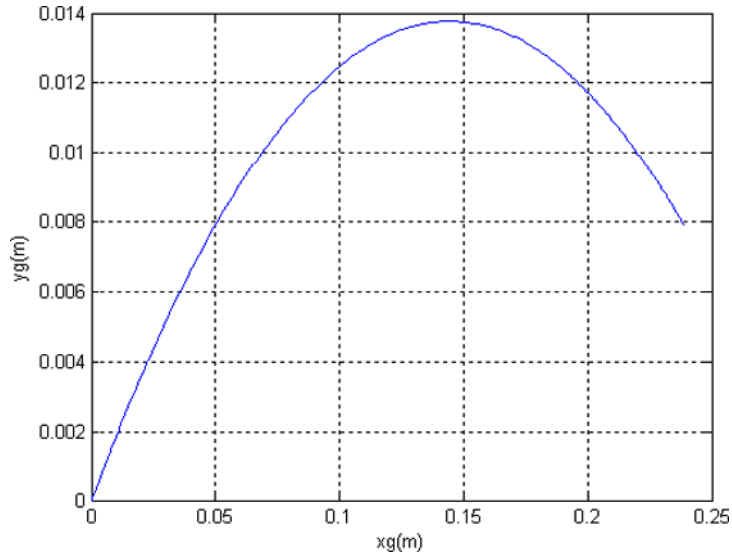

Fig. 8 Curvilinear motion: trajectory of the center G

or

$$\omega_{1b}^{v}=0,\qquad \omega_{2b}^{v}=1,\qquad \omega_{10b}^{v}=-\frac{r}{l},$$
$$\omega_{3b}^{v}=\frac{R}{r_0}\omega_{10b}^{v},\qquad \omega_{\varphi b}^{v}=-\omega_{10b}^{v}, \tag{34}$$

two plots for the torques of equal magnitudes and opposite signs (Fig. 6) and the powers (Fig. 7) of the right and left driving wheels for pure rotation about the centerline of the wheel axle, are displayed versus time during $\Delta t=3$ s. The irregularities in the graphs of torques during the first 0.85 s correspond just to the period of transition to the stabilized rotation motion.

Considering the masses of the caster wheel and the crank negligible, the torque applied at the axle of each driving wheel is given by following relation:

$$M_1=|M_2|$$
$$=\left[2\frac{r^2}{l^2}\left(J_1^z+m_1a^2\right)+m_2^A r^2\left(\frac{3}{2}+\frac{r^2}{l^2}\right)\right]\ddot{\theta}_1. \tag{35}$$

3. *Curvilinear motion*: $\theta_2^*=2\theta_1^*=\frac{\pi}{2}$. If the platform's center Gmoves along a curvilinear trajectory (Fig. 8), the time-history of the torques (Fig. 9) and powers (Fig. 10) exerted by the actuators A_2, B_2 can be calcu-

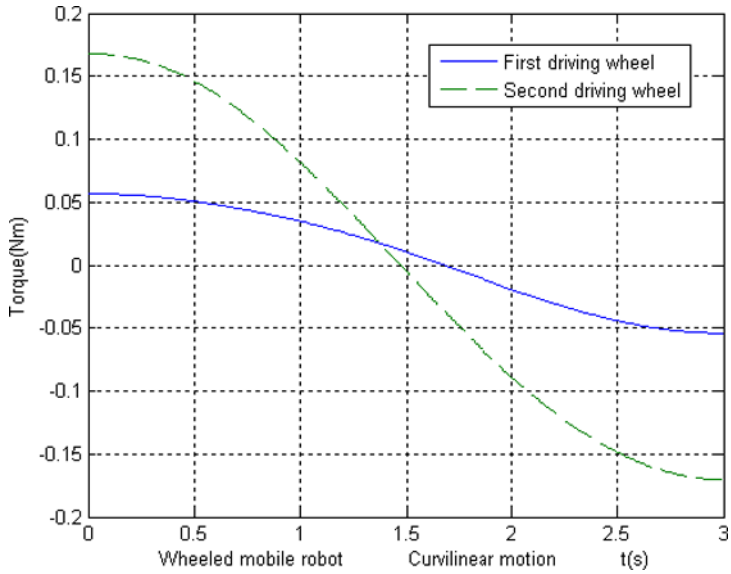

Fig. 9 Curvilinear motion: torques of driving wheels

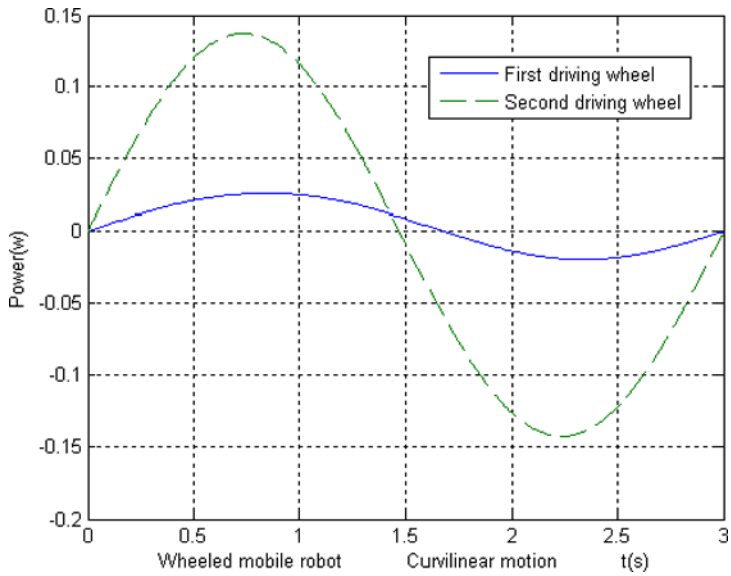

Fig. 10 Curvilinear motion: powers of driving wheels

lated with the computer program, using the MATLAB software.

5 Conclusions

1. The paper analyzed the direct kinematics and inverse dynamics of a mobile robot provided with caster wheel.
2. The numbers of relations given by the Lagrange equations is equal to the total number of the position variables and Lagrange multipliers inclusive. Also, the analytical calculations involved in these equations present an elevated risk of errors. So, applying the Lagrange formalism we obtain 12 equations, while the Newton–Euler classic method brings to a system of 36 equations.
3. Within the forward kinematics analysis, some exact relations that give in real time the velocity and acceleration of each element of the wheeled mobile robot have been established in the present paper. The dynamics model takes into consideration the mass, the tensor of inertia and the action of weight and inertia forces introduced by each element of the

robot. Some modeling methods for robot dynamics neglect the influence of these factors.

4. The dynamics of this mechanical system is formulated using the fundamental principle of virtual work, but the results in the framework of the Lagrange equations with their multipliers have been *verified*.
5. Neglecting the friction forces and considering the gravitational effects, the new approach can eliminate all forces of internal joints and give a direct determination of the time-history evolution of torques and powers required by the two driving wheels. The simulation through the software MATLAB program certifies that one of the major advantages of the current matrix recursive formulation is a reduced number of additions or multiplications and consequently a smaller processing time of numerical computation in comparison with the approach based on the Lagrange equations. Relations (15), (17) represent two complete explicit equations of the dynamic simulation and, in a context of automatic command, can easily be transformed into a robust model for computerized control of the mobile robot provided with caster wheels.

References

1. Agulló, J., Cardona, S., Vivancos, J.: Kinematics of vehicle with directional sliding wheels. Mech. Mach. Theory **22**(4), 295–301 (1987)
2. Abou-Samah, M., Krovi, V.: Cooperative frameworks for multiple mobile robots. In: CCToMM Symposium on Mechanisms, Machines and Mechatronics, Canadian Space Agency (Saint-Hubert) Montréal, Canada (2001)
3. Muir, F.P., Neuman, C.P.: Kinematic modeling of mobile robots. J. Robot. Syst. **4**(2), 281–304 (1987)
4. Angeles, J.: Fundamentals of Robotic Mechanical Systems: Theory, Methods and Algorithms. Springer, New York (2002)
5. Colbaugh, R., Trabatti, M., Glass, K.: Redundant Non-Holonomic Mechanical System. Characterization and Control. Robotica, vol. 17. Cambridge University Press, Cambridge (1999)
6. Kim, Y.H., Lewis, F.L., Abdallah, C.T.: A dynamic recurrent neural-network based adaptive observer for a class of non-linear systems. Automatica **33**(8), 1539–1543 (1997)
7. Giergiel, J., Zylski, W.: Description of motion of a mobile robot by Maggie's equations. J. Theor. Appl. Mech. **43**(3), 511–521 (2005)
8. Hendzel, Z.: An adaptive critic network for motion control of a wheeled mobile robot. Nonlinear Dyn. **50**(4), 849–855 (2007)
9. Velinski, S.A., Gardner, J.F.: Kinematics of mobile manipulator and implications for design. J. Robot. Syst. **17**(6) (2000)
10. Papadopoulos, E., Poulakakis, E.: On motion planning of nonholonomic mobile robots. In: Proceedings of the International Symposium on Robotics, Montréal, Canada, pp. 77–82 (2000)
11. Carricato, M., Parenti-Castelli, V.: Singularity-free fully-isotropic translational parallel mechanisms. Int. J. Robot. Res. **21**, 2 (2002)
12. Merlet, J.P.: Parallel Robots. Kluwer Academic Press, Dordrecht (2000)
13. Pathak, K., Franch, J., Agrawal, S.K.: Velocity and position control of a wheeled inverted pendulum by partial feedback linearization. IEEE Trans. Robot. **21**(3), 505–513 (2005)
14. Gracia, L., Tornero, J.: Kinematic modelling and singularity of wheeled mobile robots. Adv. Robot. **21**(7), 793–816 (2007)
15. Chakraborty, N., Ghosal, A.: Kinematics of wheeled mobile robots on uneven terrain. Mech. Mach. Theory **39**(12), 1273–1287 (2004)
16. Chakraborty, N., Ghosal, A.: Dynamic modelling and simulation of a wheeled mobile robot for traversing uneven terrain without slip. J. Mech. Des. **127**(5), 901–909 (2005)
17. Salerno, A., Angeles, J.: On the nonlinear controllability of a quasiholonomic mobile robot. In: Proceedings of the IEEE International Conference on Robotics & Automation ICRA'2003, Taipei, Taiwan, pp. 3379–3384 (2003)
18. Salerno, A., Ostrovskaya, S., Angeles, J.: The dynamics of a novel rolling robot-analysis and simulation. In: Proceedings of the 11th World Congress in Mechanism and Machine Science, Tianjin, China, pp. 1956–1960 (2004)
19. Staicu, S., Zhang, D., Rugescu, R.: Dynamic modelling of a 3-DOF parallel manipulator using recursive matrix relations. In: Robotica, vol. 24, pp. 125–130. Cambridge University Press, Cambridge (2006)
20. Staicu, S., Liu, X.J., Wang, J.: Inverse dynamics of the HALF parallel manipulator with revolute actuators. Nonlinear Dyn. **50**(1–2), 1–12 (2007)
21. Staicu, S., Zhang, D.: A novel dynamic modelling approach for parallel mechanisms analysis. Robot. Comput. Integrated Manuf. **24**(1), 167–172 (2008)
22. Staicu, S., Carp-Ciocardia, D.C.: Dynamic analysis of Clavel's delta parallel robot. In: Proceedings of the IEEE International Conference on Robotics & Automation ICRA'2003, Taipei, Taiwan, pp. 4116–4121S (2003)
23. Staicu, S.: Inverse dynamics of a planetary gear train for robotics. Mech. Mach. Theory **43**(7), 918–927 (2008)
24. Staicu, S.: Relations matricielles de récurrence en dynamique des mécanismes. Rev. Roum. Sci. Tech. Sér. Méc. Appl. **50**(1–3), 15–28 (2005)
25. Tsai, L.W.: Robot Analysis: The Mechanics of Serial and Parallel Manipulators. Wiley, New York (1999)